

Weighing 40 X-ray Luminous Clusters of Galaxies with Weak Gravitational Lensing

H. Dahle

Institute for Astronomy, University of Hawaii

Abstract. Deep two-color imaging of 40 clusters of galaxies with the NOT and the University of Hawaii 2.24-m telescope is used to measure the weak gravitational shear acting on faint background galaxies. From this, maps of the projected cluster mass distribution are constructed, and the cluster masses are measured within circular apertures of up to $\sim 3h^{-1}$ Mpc. The results are used to derive the cluster mass function at $z \sim 0.2$. The average mass-to-light ratio of the clusters indicate a low-density Universe with $\Omega_0 \simeq 0.25$. Additional mass concentrations are found along the lines of sight to the clusters, some of which are most likely associated with clusters at $z > 0.5$. In addition, the data are used to measure weak gravitational lensing due to large-scale structures along the line of sight. The future prospects for this kind of research with the NOT are briefly discussed.

1. Introduction

The weak gravitational lensing phenomenon has for a decade been used to probe the dark matter distribution in the Universe on scales ranging from galaxies to large-scale structures. Rapid progress has been made both observationally and theoretically, and many important developments have taken place only during the last 2-3 years. Much of the progress on the observational side is due to the development of large-format (usually mosaic) CCD cameras which can cover fields of order 0.5 degrees on a side on 4-meter class telescopes. Such cameras are currently among the most heavily used instruments at leading observatories, and significant resources are being spent on building even larger CCD mosaics. Weak lensing studies are frequently mentioned as an important part of the scientific motivation for these technical developments.

On the theoretical side, many different inversion algorithms for reconstructing the mass distribution from measurements of weak gravitational shear have been developed, e.g. to take into account strong lensing in the inner regions of the clusters. With the increase in the size of CCD cameras, weaker and weaker shear can in principle be measured, provided that systematic effects can be kept under control. Recently developed algorithms can account for the effects of realistic PSFs and optimally weigh background galaxies of different fluxes, shapes and sizes when estimating the weak shear.

Why all the interest in weak lensing? For the first time, we are getting an unbiased (although still fairly noisy) look at the mass distribution in the Universe. We are now at a stage where measurements are getting sufficiently sensitive to map the projected mass distribution along any line of sight. In many ways, this is similar to what happened in the past when new parts of the electromagnetic spectrum became available for astrophysical studies, but the mass probed by lensing is a much more fundamental quantity than electromagnetic radiation emission and this makes weak

lensing measurements a very powerful tool for distinguishing between different models for structure formation.

2. The cluster sample

Our observational efforts at the NOT have been focused on measuring weak gravitational shear in cluster fields. Although many weak lensing studies over the past decade have targeted clusters of galaxies – see e.g. the recent reviews by Mellier (1999) and Bartelmann & Schneider (2000) and references therein – they have mostly been limited to studies of a few clusters which are thought to be extremely massive, thereby guaranteeing a significant weak lensing signal. Until now, there has been no weak lensing study of a large, well-defined sample of objects. The sample described here was selected from the lists of X-ray luminous clusters published by Briel & Henry (1993), Ebeling et al. (1996; XBACS) and Ebeling et al. (1998; BCS). The clusters are in the redshift range $0.15 < z < 0.35$ and almost all have X-ray luminosities $L_{X,0.1-2.4\text{keV}} \geq 10^{45} \text{ erg s}^{-1}$ (for $h = 0.5$, $q_0 = 0.5$). Most of the clusters are targets for recent or planned X-ray observations with Chandra or XMM-Newton.

3. Observations and reduction

The NOT observations were made with ALFOSC in imaging mode, and 1.5h of exposure was typically obtained for each cluster in each of the V- and I-bands. Additional observations were made with the University of Hawaii 2.24-m telescope at Mauna Kea Observatory with either a 2k Tektronix CCD camera or the UH8K CCD mosaic (Luppino et al. 1995). The UH8K pixels were 2×2 re-binned to effectively make a 4k detector with a $19'$ field. To avoid introducing artificial shape distortions mimicking the effect of weak lensing, the individual exposures had to be accurately aligned to produce a deep combined exposure of each field. For the 2k data, catalogs of stellar positions was generated for all exposures, and an exposure with minimal extinction was chosen to be the astrometric and photometric reference for the other exposures. A least-squares solution was then calculated for a lower-order polynomial astrometric transformation of each exposure into the reference, and the images were median combined into a final image. To eliminate artificial galaxy shape distortions due to PSF anisotropies, a spatially variable PSF model was calculated, and the image was convolved with the model, rotated by $\pi/2$, to yield a smoothed image with a nearly circular PSF. The PSF model, along with the combined image and the smoothed image, was used to estimate the gravitational shear acting on a sample of faint background galaxies in the field with optimized weighting of the galaxies as a function of their fluxes, sizes and shapes (for details on the shear estimator, see Kaiser 2000).

The 8k data were reduced using a procedure very similar to the one described by Kaiser et al. (1999). An astrometric solution was found which accounts for the CCD chip layout in the camera and field distortions (which were quite small), using the USNO-A2.0 catalog as a reference. The PSF is known to vary discontinuously across chip boundaries in the UH8K camera, so the individual chip frames were convolved with a re-circularizing filter generated as described above before combining the frames. A set of ‘raw’ and ‘re-circularized’ combined images were then made, and the shear was estimated in essentially the same way as for the 2k data.

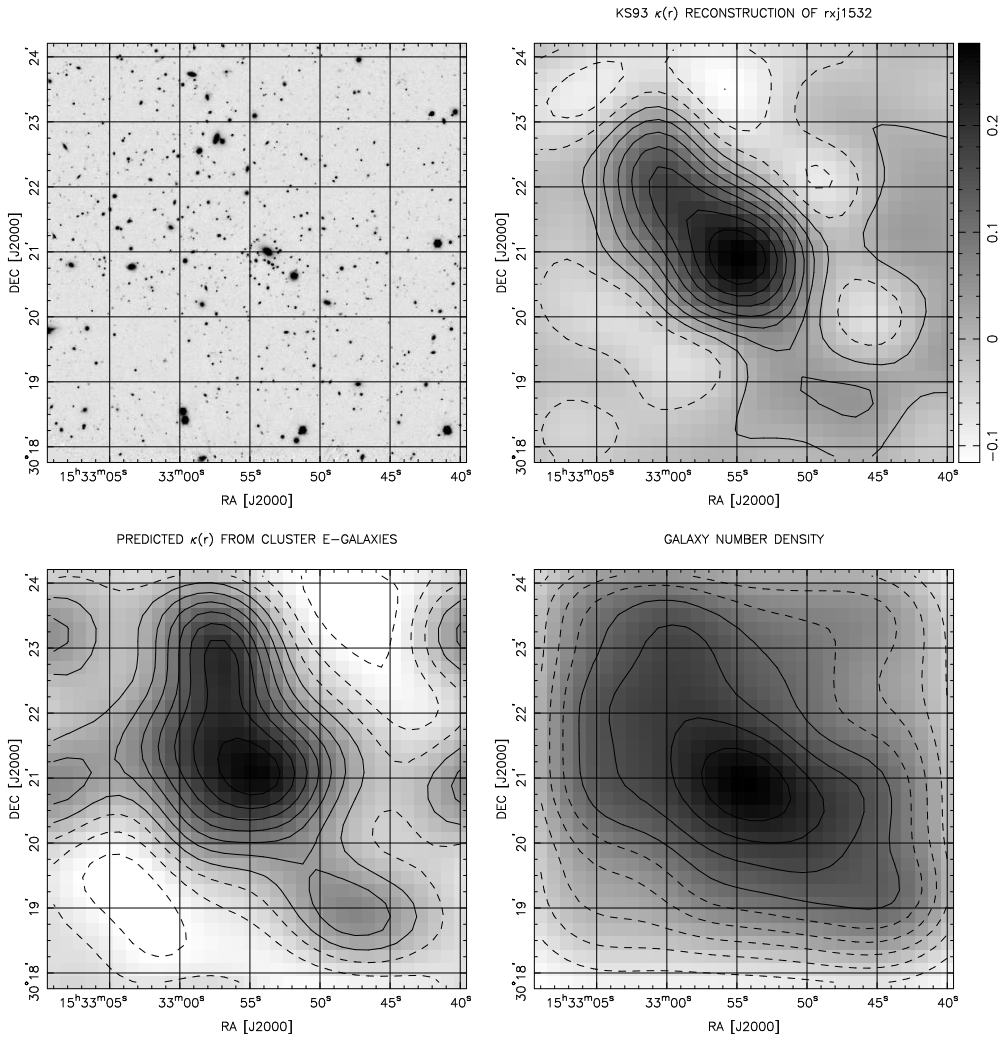


Figure 1. The upper left panel shows an I -band image of the cluster RXJ1532.9+3021 ($z=0.345$), based on 3 hours of exposure with ALFOSC in May 1999. The upper right panel shows the projected mass density in the field, calculated from weak lensing measurements. The lower left panel shows the predicted mass density, based on photometry of early-type cluster galaxies, and the lower right panel shows the number density of galaxies in the field. The contour plots have all been smoothed with a Gaussian of scale $36''$, and the average value has been subtracted from the two lower plots.

4. Weak Lensing Analysis

4.1. Predicted and reconstructed surface density

Using local measurements of the spectral energy distributions (SEDs) of galaxies of different types (Coleman et al. 1980), and assuming negligible galaxy color evolution, it is possible to predict the broadband colors of galaxies as a function of redshift. Lubin (1996) shows that the colors of early-type galaxies at redshifts $z < 0.4$ are well represented by this no-evolution prediction. In this redshift range, early-type galaxies can be separated by their V-I colors from spirals and irregulars, and early-type galaxies in rich clusters form a tight, well-defined sequence in color-magnitude space. It is thus fairly easy to identify and isolate the early-type cluster galaxies and other early-type galaxies at moderate redshifts. Assuming that the mass traces the early-type galaxies with a constant mass-to-(early type galaxy) light ratio, a map of the predicted mass distribution in the field can be generated and compared to the mass distribution derived from weak lensing. The projected surface density was reconstructed from the shear measurements using the algorithm of Kaiser & Squires (1993), which is fast to implement and has well-understood noise properties. An example of the results for the cluster RXJ1532.9+3021 is shown in figure 1.

4.2. Light-mass cross-correlation

To investigate the relative distribution of mass and galaxy light in the field, the two-dimensional cross-correlation between the measured and predicted mass distribution was calculated. This was compared to the auto-correlation of the predicted mass distribution from galaxy photometry. The results of this procedure when applied to wide-field data is particularly interesting, since they probe a wide range of physical radii in the clusters. The clusters display a range of properties: In some clusters, the dark matter appears to be significantly more concentrated than the early-type galaxy light, in others the two components trace each other within the errors, and in some clusters the mass is significantly more extended than the light. The differences appear to be related to the dynamical state of the clusters. The clusters which appear to be completely relaxed systems have the more concentrated dark matter distributions, whereas the clusters with the more extended dark halos appear to still be in the later stages of their formation process.

The rest-frame B-band mass-to-light ratios in the cluster fields were calculated by taking the discrete Fourier transform of the predicted and measured surface density images and comparing the amplitudes of the Fourier modes. In figure 2, the resulting values for M/L_B are plotted against the physical scale corresponding to the longest wavelength measured. Also plotted are a number of other M/L_B measurements taken from the literature (Bahcall et al. 1995). The average value for the observed clusters is $M/L_B = 377 \pm 17$ in solar units, which coupled with local measurements of the B-band luminosity density (Loveday et al. 1992) indicates a value for the density parameter of $\Omega_0 \simeq 0.25$.

4.3. Comparison with other mass measurements

Many of the clusters in the sample studied here have X-ray temperature measurements and/or galaxy velocity dispersion measurements available. By fitting a singular isothermal sphere model to the measured tangential shear profiles around the clusters, the weak lensing measurements can be compared to velocity dispersion measurements, as shown in figure 3. The agreement is generally fairly good, with a tendency for the

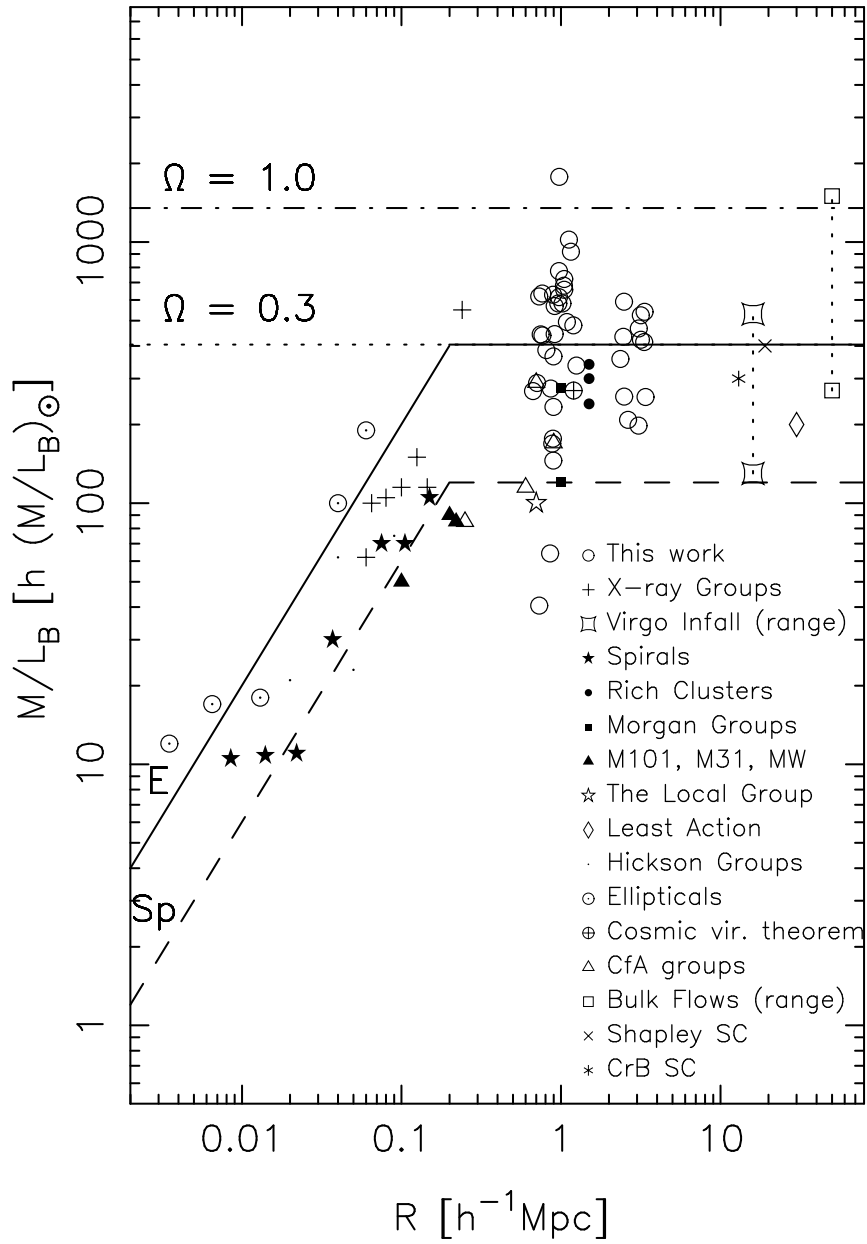


Figure 2. (Rest-frame) B -band mass-to-light ratio vs. physical scale. The M/L_B expected for $\Omega = 1$ and $\Omega = 0.3$ are shown as lines, along with empirical fits to M/L_B (assumed to increase proportional to R up to a scale of $100h^{-1}$ kpc) for spirals and ellipticals. The plotted points for rich clusters, Morgan groups, Hickson groups, CfA groups, spirals and ellipticals are median values of these samples. The circles are values for the clusters studied in this work, using the mass to total light ratio. The figure is in part based on a similar plot by Bahcall et al. (1995). See this paper for further references.

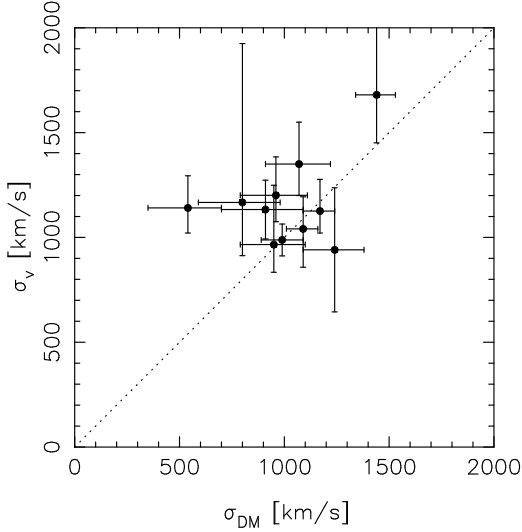


Figure 3. Spectroscopically measured velocity dispersion σ_v vs. the dark matter velocity dispersion σ_{DM} , inferred from weak lensing measurements.

spectroscopically measured velocity dispersion to be marginally larger than the dark matter velocity dispersion (derived from the weak lensing measurements) for about half of the clusters. This is not unexpected, since the spectroscopically measured velocity dispersions may be biased upwards due to line-of-sight contamination by galaxies in the infall region outside the virial radius of the clusters.

4.4. The mass function of galaxy clusters

From the list of observed clusters, a volume-limited BCS subsample with the selection criteria $0.1 < z < 0.25$ and $L_{\text{X},0.1-2.4\text{keV}} \geq 10^{45} \text{ erg s}^{-1}$ was selected. Using the singular isothermal sphere model fit, the masses contained within the inner $0.5h^{-1}$ Mpc of the clusters were calculated, and a cumulative cluster mass function was constructed, as shown in figure 4. This is the first mass function of galaxy clusters which is based on gravitational lensing measurements. Further work is currently in progress to compare the results to predictions from Press-Schechter theory and from recent large cosmological N-body simulations (e.g. Jenkins et al. 2000).

4.5. Detection of additional mass concentrations along the line of sight

In addition to the targeted clusters, some additional mass concentrations are seen in the reconstructed density maps of some cluster fields. These mass concentrations tend to be associated with concentrations of red ($V - I > 2.2$), faint galaxies, which indicates that they are distant clusters ($z > 0.5$). One distant cluster candidate, situated in the field of Abell 1705, even shows a strongly lensed blue arc surrounding what appears to be the central cluster galaxy (see figure 5). Thus, the weak lensing measurements can be used to discover new clusters in the observed fields. The availability of color information is a great help in this respect: What initially appeared as a ‘dark cluster’ in the field of Abell 1722, similar to the one reported by Erben et al. (2000), turned out to be associated with a concentration of red galaxies which did not stand out from the background/foreground in data from a single passband only.

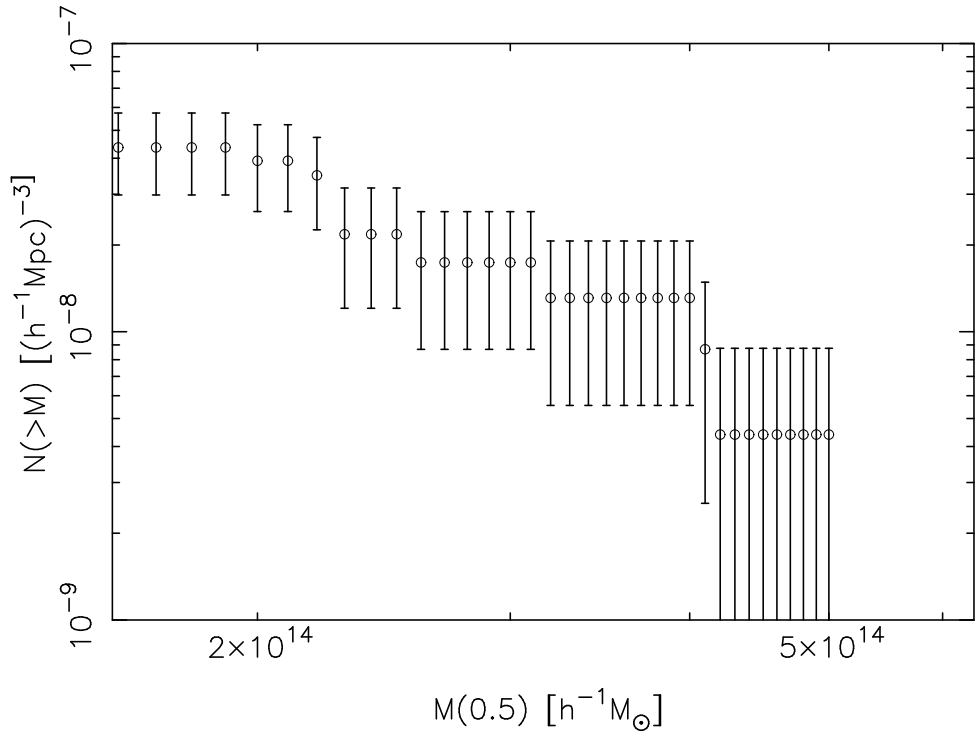


Figure 4. Cluster mass function. The quantity $M(0.5)$ is the mass within a cluster radius of $0.5 h^{-1} \text{Mpc}$ in three-dimensional space.

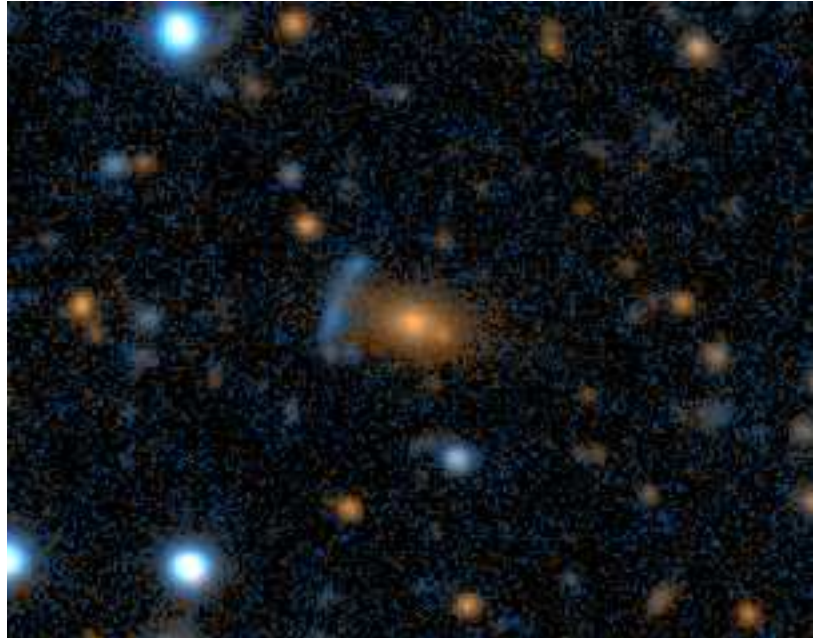


Figure 5. A blue arc curving around the central galaxy of a previously unknown, distant cluster.

4.6. Cosmic shear in cluster fields

Several groups have recently reported the detection of weak cosmic shear from large-scale structures along the line of sight (Bacon et al. 2000; Kaiser, Wilson & Luppino 2000; van Waerbeke et al. 2000, Wittman et al. 2000). These studies are generally based on observations of ‘blank fields’ not containing any previously known clusters. The presence of the massive clusters in the imaging data described here may bias the cosmic shear measurement somewhat, but the shear on different sides of the cluster (which is generally situated near the center of each field) will mostly cancel out, and measurements of the net shear across the image will thus only be weakly affected by the presence of the cluster. Using 12 cluster fields observed in the I-band with the UH8K camera, the cosmic shear variance on scales of $20'$ was measured to be $\langle \bar{\gamma}^2 \rangle_{II} = 1.24 \pm 0.49 \times 10^{-4}$, consistent with the results of Wittman et al., but marginally larger than the Kaiser et al. result. Using a cross-correlation of shear measurements from I-band data and shallower V-band data in 7 UH8K fields (which will cancel out systematic effects which are not common to both passbands), an upper limit of $\langle \bar{\gamma}^2 \rangle_{IV} < 0.50 \times 10^{-4}$ was derived, more in line with the values found by Kaiser et al.

5. Future prospects: What NOT can (and can’t) do

Although the Mosaic/FRED combination would still be extremely competitive if both instruments were already available, the NOT will within a couple of years become less attractive for weak lensing studies requiring very wide fields (e.g. measurements of cosmic shear and weak galaxy-galaxy lensing), since the field sizes of competing facilities (such as Subaru Suprime-Cam, CFHT MegaPrime, MMT Megacam, VST and VISTA) are rapidly increasing. In the more distant future, wide-field weak lensing observations will most likely be carried out using dedicated facilities such as the proposed Dark Matter Telescope (see <http://www.dmt telescope.org>) or an array of smaller telescopes (Kaiser, Tonry & Luppino 2000). Until then, the NOT (with Mosaic/FRED) will likely remain competitive for weak lensing observations that target a fairly large number of objects along widely separated lines of sight, such as studies of known galaxy clusters and superclusters. The main advantages of the NOT will still be the excellent intrinsic seeing at the telescope site (work to further improve image quality should have very high priority !!) and the possibility for relatively extensive telescope time allocations.

Acknowledgments. The author wishes to thank the organizers of this meeting for travel support, and he also wishes to thank Gillian Wilson for many useful discussions. The work presented here is part of a larger effort to study galaxy clusters, in collaboration with Ragnvald Irgens, Per B. Lilje, Nick Kaiser, Steve Maddox and Kristian Pedersen. The author has been sponsored by a Ph.D. research stipend awarded by Norges Forskningsråd (project number 110792/431).

References

- Bacon, D. J., Refregier, A. R., & Ellis, R. S. 2000, preprint (astro-ph/0003008)
- Bahcall, N. A., Lubin, L. M., & Dorman, V. 1995, ApJ, 447, L81
- Bartelmann, M., & Schneider, P. 2000, preprint (astro-ph/9912508)

Briel, U., & Henry, J. P. 1993, A&A, 278, 379

Coleman, G. D., Wu, C.-C., & Weedman, D. W. 1980, ApJS, 43, 393

Ebeling, H., Voges, W., Böhringer, H., Edge, A.C., Huchra, J. P. and Briel, U.G. 1996, MNRAS, 281, 799

Ebeling, H., Edge, A. C., Böhringer, H., Allen, S., Crawford, C. S., Fabian, A.C., Voges, W., & Huchra, J. P., MNRAS, 301, 881

Erben, T., Van Waerbeke, L., Mellier, Y., Schneider, P., Cuillandre, J.-C., Castander, F. J., Dantel-Fort, M. 2000, A&A, 355, 23

Jenkins, A., Frenk, C. S., White, S. D. M., Colberg, J. M., Cole, S., Evrard, A. E., & Yoshida, N., 2000, preprint (astro-ph/0005260)

Kaiser, N. & Squires, G. 1993, ApJ, 404, 441 (KS93)

Kaiser, N., Wilson, G., Luppino, G. A., & Dahle, H. 1999, PASP, in press (astro-ph/9907229)

Kaiser, N. 2000, ApJ, 537, 555

Kaiser, N., Wilson, G., & Luppino, G. A. 2000, preprint (astro-ph/0003338)

Kaiser, N., Tonry, J. L., & Luppino, G. A. 2000, PASP, 112, 768

Loveday, J., Peterson, B. A., Efstathiou, G., & Maddox, S. J. 1992, ApJ, 390, 338

Lubin, L. M. 1996, AJ, 112, 23

Luppino, G. A., Metzger, M., Kaiser, N., Clowe, D., Gioia, I., & Miyazaki, S. 1995, in "Clusters, Lensing and the Future of the Universe", ed. V. Trimble & A. Reisenegger, ASP Conf. Proc. Vol. 88, 229

Mellier, Y. 1999, ARA&A, 37, 127

Van Waerbeke, L., Mellier, Y., Erben, T., Cuillandre, J.-C., Bernardeau, F., Maoli, R., Bertin, E., Mc Cracken, H. J., Le Fèvre, O., Fort, B., Dantel-Fort, M., Jain, B., & Schneider, P. 2000, preprint (astro-ph/0002500)

Wittman, D. M., Tyson, J. A., Kirkman, D., Dell'Antonio, I., & Bernstein, G. 2000, preprint (astro-ph/0003014)